This article has been accepted for inclusion in a future issue of this journal. Content is final as presented, with the exception of pagination.

Anticipative and Predictive Control of Automated Vehicles in Communication-Constrained Connected Mixed Traffic

Longxiang Guo, *Student Member, IEEE*, and Yunyi Jia, *Senior Member, IEEE*

***Abstract*— Connected automated driving technologies have shown substantial benefits to improve the safety and efficiency of traffic. However, connected mixed traffic, which involves both connected automated vehicles and connected human-driven vehicles, is more foreseen for the realistic case in the near future. This brings new challenges because of the complexity of human elements in the system. In addition, the communication constraints in realistic connectivity such as random delays and packet losses bring even more challenges to the system. Therefore, this paper proposes a new anticipative and predictive automated vehicle control approach in connected mixed traffic. The approach first anticipates the states of surrounding vehicles including human-driven vehicles, and then integrates the anticipation into the predictive control of automated vehicles, which can help improve the control performance and also handle the communication constraints. An inverse model predictive control (IMPC) based anticipation approach has been proposed. The proposed approach, together with constant speed (CS), intelligent driver model (IDM) and artificial neural network (ANN) based anticipation methods are integrated with model predictive control (MPC) for automated vehicle control. The approaches have been tested in human-in-the-loop experiments and the results show that the integration with a newly proposed IMPC based anticipation has shown the best performance in terms of accuracy, efficiency and scalability in connected mixed traffic with both ideal and constrained communications.**

***Index Terms*— Human driving behaviors, inverse model predictive control, learning and prediction, connected mixed traffic.**

I. Introduction

CONNECTED automated vehicle (CAV) technologies is becoming increasingly prevalent in the automobile industry. With the evolving vehicle-to-vehicle (V2V) and vehicle-to-infrastructure (V2I) communication technologies, CAVs can bring many benefits in various of environments. In urban environments, CAVs can reduce traffic jams and increase road and intersection capacity [1], [2] by sharing traffic and road infrastructure information. They can also improve driving safety around corners by enhancing situational awareness capability [3]. On highways, CAVs can save energy by reducing aerodynamic drag and increasing road capacity [4]. By sharing vehicle states, CAVs also help reduce the risk of collision during emergent braking [5] and lane switching [6].

However, realizing the full potential of the aforementioned benefits requires seamless communication and perfect control of each vehicle. Communication constraints, due to their randomness, pose the biggest challenge to CAVs. They change the dynamics of the platoon markedly [7], [8]. The string stability of a platoon can be seriously compromised by communication delays [9], [10], impacting both safety and efficiency of the fleet. Some studies have tried to solve this problem by implementing different controller designs. H-infinity control [11] and other robust controllers are used to resist communication delays. Some other researchers have proposed methods to estimate communication delays [12]. Although robust controllers can regain string stability, control error still increases significantly with communication delay in the control loop [13]. For optimal controllers, the estimated delays can be directly incorporated in the prediction model [14], and the output of the controller can be compensated using available timestamps [15]. In recent years, predictions of motions of surrounding vehicles are used to compensate for delays in the control of homogeneous automated vehicle platoons [22]–[26]. However, existing approaches still do not provide a comprehensive analysis of the tradeoffs between safety, stability and efficiency, and comfort. Handling random communication constraints in connected automated driving still remains a problem.

Connected mixed traffic (CMT) is posing extra challenges compared to CAVs. In CMT, human-driven vehicles (HDV) will be mixed with automated vehicles (AV), which is going to be a common situation in the near future. Unlike AVs, HDVs are not controlled by computers, and their current actions are not available to be shared. Therefore, AVs need to find another method to know how HDVs behave and then adapt to them. Therefore, predicting the behaviors of HDVs is critical, especially under communication constraints.

This paper will focus on the longitudinal control of CMT. To solve the HDV prediction problem, a suitable human driver model needs to be built for anticipation. Car following models such as the Tampère (TMP) model [16], Optimal Velocity Model (OVM) [17], and Intelligent Driver Model (IDM) [18] have been proposed. The limitations of these models are their simple structure and original objective, which is generation of smooth control outputs. The latter particularly renders them unsuitable for making predictions about an individual

Manuscript received May 20, 2020; revised November 3, 2020; accepted February 17, 2021. This work was supported in part by the National Science Foundation under Grant CNS-1755771 and Grant IIS-1845779. The Associate Editor for this article was N. Bekiaris-Liberis. *(Corresponding author: Yunyi Jia.)*

The authors are with the Department of Automotive Engineering, Clemson University, Greenville, SC 29607 USA (e-mail: longxig@clemson.edu; yunyij@clemson.edu).

Digital Object Identifier 10.1109/TITS.2021.3067282

1558-0016 © 2021 IEEE. Personal use is permitted, but republication/redistribution requires IEEE permission.
See https://www.ieee.org/publications/rights/index.html for more information.

Authorized licensed use limited to: CLEMSON UNIVERSITY. Downloaded on July 11,2021 at 01:17:18 UTC from IEEE Xplore. Restrictions apply.

This article has been accepted for inclusion in a future issue of this journal. Content is final as presented, with the exception of pagination.

HDV. In the recent years, many data-driven machine learning approaches have been proposed to model the behaviors of a human driver. The most popular ones are Artificial Neural Networks (ANN) based approaches [19]–[21]. However, these approaches require a large set of carefully prepared data to train the network parameters. More importantly, the scalability of such approaches is limited by the scenarios covered by the training data. Consequently, they find it difficult to handle never-seen situations.

Our previous work [27] has proposed an inverse model predictive control (IMPC) based prediction for human-driven vehicles. The novelty of this work when compared to the previous paper is the further expansion of the IMPC formulation for solving more complex control problems that involve automated vehicles in connected mixed traffic. In addition, we have also extended the application of IMPC to cope with potential communication constraints in connected mixed traffic. The IMPC's capability in helping the predictive controls to resist communication constraints is compared with other existing approaches to illustrate the advantages. The major contributions can be summarized as follows.

1. Proposes a new anticipative and predictive automated vehicle control approach in connected mixed traffic based on the anticipation of surrounding vehicles' states including human-driven vehicles and predictive control of automated vehicles.
2. Propose a different anticipation approach to anticipate the states of human-driven vehicle, especially including the IMPC based approach which can achieve better anticipation accuracy and scalability.
3. Conduct human-in-the-loop experiments to conclude that the proposed anticipative and predictive automated vehicle control with the proposed IMPC based anticipation can achieve the best control performance in terms of safety, accuracy, efficiency, and comfort under both ideal and constrained communications in connected mixed traffic.

The rest of the paper is organized as follows. Section II introduces predictive control of automated vehicles in connected traffic. Section III presents the experimental design and the analysis of results.

II. Anticipative and Predictive Automated Vehicle Control

The framework for anticipative and predictive control of automated vehicles is described in II-A. The details of predictive control of automated vehicles in connected traffic is introduced in II-B. The comparison of anticipation methods, especially the IMPC based predictor, is presented in II-C. Finally, II-D discusses how the communication constraints are handled by the proposed methods.

A. Anticipative and Predictive Control Framework

In connected mixed traffic, every vehicle including the HDV shares information with every other vehicle. With anticipative and predictive control, vehicles need to share not only their instantaneous states, but also their entire anticipated trajectories for the near future. Each AV in the traffic utilizes the shared information in the predictive controller to better plan the driving task and control the motion. The structure of the anticipative and predictive control in connected mixed traffic is shown in Fig. 1.

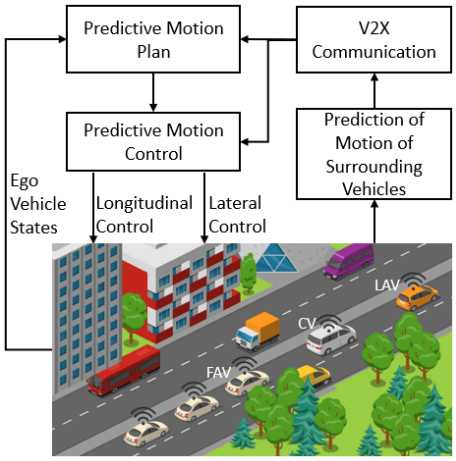

Fig. 1. Framework of anticipative and predictive control.

In the framework, each vehicle measures the states of itself and the vehicles that are right next to it using the available sensors. The measured states are being used to generate predictions about the future motion of the ego vehicle. The predictions are then shared through V2V and V2I communications with other vehicles. With the help of the predictions, AVs can react way faster to events that are likely to happen in the immediate future. AVs can plan ahead to avoid unnecessary brakes and improve riding comfort and energy efficiency, or to brake early to reduce the risks of the predicted situation evolving into an accident. Communication delays and packet losses together forms a combined delay. A large combined delay compromises the benefits of V2V and V2I communications. In such cases, the more precise the prediction is, the less the predictive controller will be affected since the AVs can still use the previously received predictions easily by shifting the predicted motion trajectory by the estimated combined delay.

In this paper we are applying the proposed framework to the longitudinal car following control problem in connected mixed traffic. Without loss of generality, we have selected the most representative mixed traffic problem which can be generalized into a three-car scenario. The lead car is an automated vehicle (LAV) that is either free-flowing or at the end of a full AV platoon. The center vehicle (CV) is an HDV that separates two AV platoons. The following car is another automated vehicle (FAV) that follows the CV. LAV is neither communicated to CV nor affected by CV, so the anticipative and predictive control is mainly applied to the FAV.

B. Anticipative and Predictive Automated Vehicle Control

In this paper we chose to use MPC as the controller since it can find the optimal control solution given the predicted states of the HDV. The rest of this section will introduce details about the MPC for the AVs.

Authorized licensed use limited to: CLEMSON UNIVERSITY. Downloaded on July 11,2021 at 01:17:18 UTC from IEEE Xplore. Restrictions apply.

This article has been accepted for inclusion in a future issue of this journal. Content is final as presented, with the exception of pagination.

1) Model of Automated Vehicles: The system model used in the FAV's MPC is a linear time invariant (LTI) model with a first order lag with time constant τ [28]:

$$\begin{bmatrix} \dot{s_f} \\ \dot{v_f} \\ \dot{a_f} \end{bmatrix} = \begin{bmatrix} 0 & 1 & 0 \\ 0 & 0 & 1 \\ 0 & 0 & -\frac{1}{\tau} \end{bmatrix} \begin{bmatrix} s_f \\ v_f \\ a_f \end{bmatrix} + \begin{bmatrix} 0 \\ 0 \\ \frac{1}{\tau} \end{bmatrix} u_f \tag{1}$$

where s_f, v_f, a_f and u_f are the travelled distance, speed, acceleration, and control input of the automated vehicle respectively. The physical meaning of u_f is desired acceleration.

In the simulation, the plant model of FAV shares the same form as the system model (1). Using such an LTI model as plant model is acceptable in this paper since later all different predictors share this same plant model. Thus, the effects of inaccuracy in modelling vehicle dynamics can be ignored. The plant model of the automated vehicle differs from the system model in terms of the use of different time constants. Due to the differences in the dynamics of the powertrain and the brake systems, the time constant differs during braking and acceleration. While the powertrain system has a large time constant of $\tau_p = 0.45s$, the braking system has a smaller time constant of $\tau_b = 0.1s$. The system model in the MPC uses the mean time constant $\tau_m = 0.275s$. Assuming that the road is flat, the switching between τ_p and τ_b is governed by the drive force F_w that acts on the wheels:

$$\tau = \begin{cases} \tau_p, & F_w \geq 0 \\ \tau_b, & F_w < 0 \end{cases},$$
$$F_w = m_{eff} u_f + \frac{1}{2}\rho_a A_f C_d v_f^2 + \mu m g \tag{2}$$

The drive force F_w is calculated using the desired acceleration u_f. While a negative value of F_w means that the brake needs to be applied, a positive value of F_w means that the throttle needs to be applied. The parameters that are used to calculate F_w are shown in Table I. The parameters were determined based on [28].

2) Model Predictive Longitudinal Control of Automated Vehicles: Due to the advantage of MPC, a variety of objectives can be desired in MPC for the FAV based on different requirements. In this paper, in order to make the performance comparison between different predictors clearer and more direct, without any loss of generality, the objective is designed as maintaining a constant headway distance d_f^{ref}, which is a common and critical requirement in connected automated driving. The cost function can be then written as:

$$J_f = \sum_{\kappa=k}^{k+N} [w_d \left(d_f(\kappa) - d_f^{ref}\right)^2 + w_a a_f(\kappa)^2 + w_u u_f(\kappa)^2] \tag{3}$$

where d_f is the spacing between the ego CAV and the preceding vehicle, N is the number of prediction steps, w_d, w_a and w_u are the corresponding weights. The optimal control can be obtained by solving the constrained optimization:

TABLE I
PLANT PARAMETERS

Parameter	Definition	Value
m_{eff}	Effective Mass	1706.9kg
m	Mass	1671kg
μ	Rolling Resistance Coefficient	0.01
g	Acceleration of Gravity	$9.81 m/s^2$
ρ_a	Air Density	$1.225 \text{kg}/m^3$
C_d	Aerodynamic drag coefficient	0.29
A_f	Vehicle Frontal Area	$2.733 m^2$

$$\begin{aligned} u_f^* = & \, arg\,min_{u_f} J_f \\ & s.t. \; -10 m/s^2 \leq a_f \leq 5 m/s^2 \\ & 0 \leq v_f \leq 40 m/s \\ & -10 m/s^2 \leq u_f \leq 5 m/s^2 \\ & d_f \geq 0 m \end{aligned} \tag{4}$$

These basic constraints are introduced to ensure feasibility and rationality of the MPC controller. Traditionally, without shared anticipation information, the MPC requires another system model for the center vehicle which is as follows:

$$\begin{bmatrix} \dot{s_c} \\ \dot{v_c} \end{bmatrix} = \begin{bmatrix} 0 & 1 \\ 0 & 0 \end{bmatrix} \begin{bmatrix} s_c \\ v_c \end{bmatrix} + \begin{bmatrix} 0 \\ 1 \end{bmatrix} a_c \tag{5}$$

This facilitates the calculation of the headway distance $d_f = s_c - s_f$ over the prediction horizon. The input a_c could be assumed to be either zero or the minimum appliable deceleration during prediction. Most of the time, the motion of the vehicle is more precisely described when $a_c = 0$. However, this can cause accidents when the center vehicle needs to brake hard. On the contrary, the minimum a_c assumption can make sure that the AV does not collide with the CV. The downside of this assumption is that it is over-conservative and significantly lowers the traffic density. In connected traffic, the shared anticipation information of the CV can give MPC the advantages of both assumptions. The anticipation information contains a set of predicted speed v_c and displacement s_c of the CV over the prediction time interval.

In this paper, we select $w_d = 1$ and $w_a = w_u = 0$ to eliminate the tuning process of the MPC. This configuration will only try to maintain the constant headway distance regardless of the control cost. The same MPC is paired with different anticipation methods and the performance indices for different predictors would be headway tracking error, vehicle acceleration and control input. The tracking error is a direct measurement of how close the controller is keeping the FAV to the control target. Vehicle acceleration can reflect how comfortable the ride in the FAV is. Moreover, when combined with control input, it also reflects how energy efficient the FAV is. While the first two statements obviously hold true, the relationships between vehicle acceleration, control input and energy efficiency need to be proven through some detailed modelling and experiments. A recent work [28] has

Authorized licensed use limited to: CLEMSON UNIVERSITY. Downloaded on July 11,2021 at 01:17:18 UTC from IEEE Xplore. Restrictions apply.

This article has been accepted for inclusion in a future issue of this journal. Content is final as presented, with the exception of pagination.

demonstrated that if the vehicle acceleration and control input can be minimized using an MPC controller then the same controller can reduce fuel consumption when applied to a very realistic simulation that includes the dynamic powertrain and transmission models. Thus, the values of the aforementioned parameters, including those in Table I and the time constants, are all determined based on [28]. In the later section where a multi-vehicle connected driving simulation is performed, if a state predictor can simultaneously reduce the average control input and the average acceleration of the FAV then it can also reduce the energy consumption.

C. Anticipation of Human-Driven Vehicle States

In this paper, the CV is an HDV. The anticipation task for a human-driven vehicle is very challenging since the control model of an HDV is unknown, and can only be learned from human driving demonstrations. Different humans may have different driving models, thus, to ensure prediction precision for HDV, we propose to make each HDV build its individual model by learning from its driving data. Each model is subsequently employed to predict the behavior of the corresponding HDV. Transmitting just motion information from LAV and HDV to FAV may not provide sufficient data for FAV to learn the individual model of each HDV. In addition, this will make the computational efforts of the FAV more complex because it will need to do the same modeling, learning and prediction process for every single HDV. Making HDV do its own prediction and share it with all other surrounding vehicles will much more efficient. Our previous work [27] has proposed an effective IMPC-based learning and modelling method for HDVs. A brief explanation of that method will be given in this section. The proposed IMPC predictor is compared with three other different predictors in this paper. Constant speed (zero a_c) predictor, which is the commonly used simple predictor in vehicle longitudinal control, is used as the performance baseline of the other predictors. According to an existing work [29], the Intelligent Driver Model and the Artificial Neural network-based predictors are doing the best in predicting human-driven vehicle states among many existing methods. Thus, in this paper the three predictors to be compared with IMPC are the CS, the IDM and the ANN predictor.

1) Constant Speed Predictor: The constant speed predictor assumes that the speed of the HDV remains unchanged during a prediction. It uses the following kinematic model to predict the motion of the human-driven vehicle:

$$\dot{s_h} = v_h \tag{6}$$

Under constant speed assumption, the FAV can directly measure the initial speed of the HDV at the start of each prediction using the onboard radar. Therefore, when the constant speed predictor is used, the FAV does not need to connect to other vehicles in the front to obtain driving information.

2) IDM-Based Predictor: Intelligent Driver Model is a widely used adaptive cruise control (ACC) model that can describe accelerations and decelerations in a satisfactory way. It has been used to simulate human driver behaviors in traffic simulation [30]. The predicted acceleration of the HDV is given by:

$$\begin{aligned} a_h &= a\left[1-\left(\frac{v_h}{v_0}\right)^4-\left(\frac{d^*}{d_h}\right)^2\right] \\ d^* &= d_0 + v_h T + \frac{v_h v_r}{2\sqrt{ab}} \end{aligned} \tag{7}$$

where $v_r = v_h - v_l$ is the predicted relative speed between the LAV and the HDV. v_0 is the desired velocity, d_0 is minimum desired spacing, T is the desired time headway, a is maximum acceleration and b is comfort braking deceleration. These 5 parameters represent the preferences of a human driver, and are the tunable/trainable parameters of this model. The IDM model is paired with the following kinematic model to predict the motion of the HDV:

$$\begin{bmatrix} \dot{s_h} \\ \dot{v_h} \end{bmatrix} = \begin{bmatrix} 0 & 1 \\ 0 & 0 \end{bmatrix} \begin{bmatrix} s_h \\ v_h \end{bmatrix} + \begin{bmatrix} 0 \\ 1 \end{bmatrix} a_h \tag{8}$$

The motion of the LAV also needs to be anticipated to complete the system model. When a human driver is driving, he/she may assume that the vehicle in the front is going to maintain its current acceleration. However, since a human driver can foresee the road situation only 0.5s-2s into the future [31], it is not realistic to keep the constant acceleration assumption through out the entire prediction process. In this paper, the duration of the entire prediction horizon is 10 seconds. While the first second of the prediction horizon uses the constant acceleration assumption, the rest of the horizon uses the constant speed assumption for the LAV, which can be described by II-C.3:

$$\begin{bmatrix} \dot{s_l} \\ \dot{v_l} \end{bmatrix} = \begin{cases} \begin{bmatrix} 0 & 1 \\ 0 & 0 \end{bmatrix} \begin{bmatrix} s_l \\ v_l \end{bmatrix} + \begin{bmatrix} 0 \\ 1 \end{bmatrix} \bar{a}_l, & \Upsilon \le 1s \\ \begin{bmatrix} 0 & 1 \\ 0 & 0 \end{bmatrix} \begin{bmatrix} s_l \\ v_l \end{bmatrix}, & \Upsilon > 1s \end{cases} \tag{9}$$

where Υ is the time within the prediction horizon, $\bar{a}_l$ is the LAV's acceleration at the start of each prediction. v_l is assumed to be constant after the prediction has passed the horizon of 1s. The predicted acceleration calculated from (7) is fed to (8), then the states of the HDV at next prediction step can be obtained. This process is repeated until a complete prediction trajectory is obtained.

The IDM model is trained using real human driving data to obtain the most suitable parameters for different drivers. The training algorithm utilizes pattern search algorithm in a high-level optimization. The optimization minimize the error between the predicted speed and headway distance, and the real speed and headway distance in demonstration.

3) ANN-Based Predictor: The ANN predictor used in this paper is based on a feed-forward structure [20] with the hidden layer having 16 sigmoidal neurons and the output layer having linear neurons. The inputs to the network are the most basic system states v_l, v_h and the system output d_h. The network is trained by fitting its output to the human demonstrated accelerations a_h^{ref}. The training data set is collected when a human drives the HDV to follow the LAV in a driving simulator. The data so collected is used by all three predictors.

Authorized licensed use limited to: CLEMSON UNIVERSITY. Downloaded on July 11,2021 at 01:17:18 UTC from IEEE Xplore. Restrictions apply.

This article has been accepted for inclusion in a future issue of this journal. Content is final as presented, with the exception of pagination.

More details about the collection of the training data will be given in Section III. The training algorithm we used is Levenberg-Marquardt method [32]. The ANN model is paired with the kinematic model given in (8) to predict the motion of the HDV.

4) IMPC-Based Predictor: The IMPC utilizes the cost function in MPC to represent a human driver's driving preferences. IMPC finds the best primitive costs to be included in the cost function and identifies the weights and references of those primitive costs to formulate the most suitable cost function dedicated to a human driver.

The HDV motion model used by IMPC is an LTI model given by (10). The LAV motion model is the same as II-C.3.

$$\begin{bmatrix} \dot{s_h} \\ \dot{v_h} \\ \dot{a_h} \end{bmatrix} = \begin{bmatrix} 0 & 1 & 0 \\ 0 & 0 & 1 \\ 0 & 0 & 0 \end{bmatrix} \begin{bmatrix} s_h \\ v_h \\ a_h \end{bmatrix} + \begin{bmatrix} 0 \\ 0 \\ 1 \end{bmatrix} u_h \tag{10}$$

The MPC problem can be formulated by minimizing a proper cost function J_h over the following prediction horizon:

$$J_h = \sum \Omega_h^T \Phi_h \tag{11}$$

where $\Phi_h = (\phi_1, \phi_2, \ldots)^T$ is a set of primitive costs for the HDV in which each element specifies the cost of a particular motion objective such as tracking the reference speed, maintaining the look-ahead distance gap and minimizing the control efforts, etc., as shown in (12), r_j is the target value of the motion objective y_j, and $\Omega_h = (\omega_1, \omega_2, \ldots)^T$ is the set of associated weights.

$$\phi_j = g\left(x_h, x_a, r_j, u_h\right) = \sum_{\kappa=k}^{k+N} \left(y_j(\kappa) - r_j\right)^2 \tag{12}$$

When a human driver is conducting a driving task, he/she may focus on and try to maintain some of the system outputs at their desired target values while leaving the rest unattended. So, we propose to evaluate the primitive costs by using each of the system outputs independently as stand-alone cost functions, which can be written as:

$$J_{\phi_j} = \phi_j = \sum_{\kappa=k}^{k+N} \left(y_j(\kappa) - r_j\right)^2 \tag{13}$$

and then learning the reference r_j with a higher-level optimization:

$$\begin{aligned} r_j^* &= arg\,min_{r_j} E \\ &s.t.:\ r_j \in C_{r_j} \end{aligned} \tag{14}$$

E is the prediction error of the MPC over a human driving demonstration. When the higher-level optimization finishes, a minimum prediction error E_{ϕ_j} over demonstrations will be obtained for the primitive cost ϕ_j. If the human driver is focusing on ϕ_j and trying to maintain y_j at a specific target value during driving, the resultant E_{ϕ_j} should be small. This means that ϕ_j can be a 'good' primitive cost in the final cost function. Otherwise, the resulted E_{ϕ_j} should be large, and ϕ_j might better be excluded from the cost function. All primitive costs can be ranked based on their E_{ϕ_j} values. We assume that $\Phi_h^* = (\phi_1^*, \phi_2^* \ldots, \phi_j^*)^T$ is the set of all available primitive costs that have been ranked from good to bad, with ϕ_1^* being the best and ϕ_j^* being the worst. Followed by this, we propose to formulate the cost function by combining the primitive costs from 'good' to 'bad', which can be described by (15).

$$\begin{aligned} J_1 &= \omega_1\phi_1^*, \\ J_2 &= \omega_1\phi_1^*, +\omega_2\phi_2^*, \\ J_3 &= \omega_1\phi_1^*, +\omega_2\phi_2^*, +\omega_3\phi_3^* \\ &\ldots. \\ J_j &= \omega_1\phi_1^*, +\omega_2\phi_2^* + \cdots + \omega_j\phi_j^* \end{aligned} \tag{15}$$

Since humans normally focus on more than one aspect during driving, it is reasonable to skip J_1 and start with a combination of the top two or three best primitive costs in the cost function first. Subsequently, in the following attempts, the next best primitive cost could be added to the cost function. Every cost function J_j will learn its parameters using higher-level optimization. Denote the set of references $r_1 \ldots r_j$ by R_j, and the set of weights $\omega_1 \ldots \omega_j$ by Ω_j, the optimization can be expressed as

$$\begin{aligned} (\Omega_j^*, R_j^*) &= arg\,min_{\Omega_h, R} E \\ &s.t.:\ \Omega_j \in C_{\Omega h}, \quad R_j \in C_R \end{aligned} \tag{16}$$

The total error E can be reduced by optimizing the weights Ω_j and the references R_j in the cost function. Since only the relative values of the weights are important, it is practical to fix one weight to 1 and optimize the rest [33]. The object function of this higher-level optimization is yet another optimization problem, however, the Jacobian of E is not obtainable. Thus, the Pattern Search (PS) algorithm [34] is adopted in this paper.

Each cost function J_j will get a minimal evaluation error E_j from the higher-level optimization. Adding an effective primitive cost ϕ_j should improve the prediction accuracy and reduce the error E_j while adding an ineffective primitive cost will not bring any benefit but affect the optimization convergence, which will result in a larger prediction error. Thus, the addition of primitive costs will be repeated until the evaluated performance of the predictor starts to deteriorate. At this point, the previous cost function can be selected to be the best cost function. It has been shown that the proposed method to select the cost-function is very effective, and the best cost function in this paper is chosen to be:

$$\begin{aligned} J_h = \sum_{\kappa=k}^{k+N} & [w_a(a_h(\kappa) - a_h^{ref})^2 + w_v(v_r(\kappa) - v_r^{ref})^2 \\ & + w_{TTCi}(TTCi_h(\kappa) - TCCi_h^{ref})^2 + w_u(u_h(\kappa) - u_h^{ref})^2] \end{aligned} \tag{17}$$

where $TTCi$ is the time to collision inverse. Three other primitive costs that have been evaluated but excluded from the cost function are the time headway inverse $THWi_h$, the headway distance d_h, and the ego vehicle speed v_h. When compared to the CS, IDM and ANN approaches, the major additional information that the IMPC incorporates is control-related information. It is difficult for the other approaches to efficiently incorporate this information because they do not have a closed-form dynamic with controls. The proposed

Authorized licensed use limited to: CLEMSON UNIVERSITY. Downloaded on July 11,2021 at 01:17:18 UTC from IEEE Xplore. Restrictions apply.

This article has been accepted for inclusion in a future issue of this journal. Content is final as presented, with the exception of pagination.

approach adopts a closed-form vehicle dynamic with MPC control which enables us to efficiently incorporate the control-related information into the cost function. Such inclusion makes the approach more complete and therefore achieve a better performance.

When the IDM, ANN or IMPC-based speed predictor is used, the FAV can only obtain the prediction information via V2V communication from the HDV. Such communication is prone to delays and packet losses.

D. Handling of Communication Constraints in Connectivity

When using V2V communication, time delays appear in the control of the automated vehicle fleet since messages need to be processed before they are transmitted between the sender and the receiver. The sender needs to sample the sensory data and process it into meaningful information. This adds processing delays to the whole process. The message will then be transmitted using certain communication protocols. During this process, the message is subject to extra processing delay, queuing delay and transmission delay. In this paper, without loss of generality, the delays between sensory data collection and anticipation generation is ignored. In order to simplify the model and the simulation process, all the other delays are merged into a single propagation delay.

Another factor that contributes to the constrains apart from the propagation delay in V2V communication is packet loss. It can be caused by errors occurring during data transmission such as network congestion. Assume that the propagation delay is Δt_{pro}, and the communication cycle is Δt_{com}. If the packet that is supposed to be delivered at $t = k\Delta t_{com}$ is successfully delivered, then the delay in the control loop at time $t = k\Delta t_{com}$ is Δt_{pro}. However, if the packet failed to reach the receiver, the controller will have to use the information from the previous communication loop at time $t = (k-1)\Delta t_{com}$. The delay in the control loop will increase to $\Delta t_{pro} + \Delta t_{com}$. If n consecutive packets are failed to be delivered, the total delay will be $\Delta t_{pro} + n\Delta t_{com}$. When the communication frequency is not high enough, packet losses can cause very large combined delays in the control loop.

In this paper, the performance of the MPC is compared with that of different predictors when propagation delays and packet losses are injected in both independent and combined manners. When communication constraints are present, the predictions received are likely to have been made a short while ago in the past, where Δt_P is the prediction step size.

$$X_P = [x_P(t-\Delta\tau), \ldots, x_P(t+n_P\Delta t_P-\Delta\tau)] \quad (18)$$

In this paper, two different cases of handling such delayed information are compared. In the first case, no global timestamp information is assumed to be available to the FAV. In other words, the FAV will treat the prediction information available at every control loop as the latest information at time t instead of at time $t-\Delta\tau$. Such unawareness does not affect the CS predictor since it is run locally. For IDM, ANN and IMPC-based predictors, the delayed prediction will be combined with on-board measurements $d_h(t)$, $a_f(t)$ and $v_f(t)$ in MPC. The mismatch of timestamps between predictions and measurements will generate unsatisfactory control input to the automated vehicle. Such a case represents the worst situation that can arise during connected automated driving.

In the second case, all vehicles are assumed to be sharing the same global time system, and the timestamps of the predictions are available to the FAV. In other words, the estimate of the combined delay time $\Delta\tau$ becomes available to the MPC controller. The whole predicted state trajectory can be shifted by $\Delta\tau$ into the future in order to match the timestamps of the current on-board measurements. The predicted states between $t+n_P\Delta t_P-\Delta\tau$ and $t+n_P\Delta t_P$ are assumed to be constant, Δt_P is the prediction step size. The detailed algorithm of this constraint-handling method is shown in Algorithm 1.

Algorithm 1 : Algorithm for Handling Communication Constraints

Input: Original prediction list $X_P(t-\Delta\tau)$
Output: Adjusted prediction list $X_P^*(t)$
for timestep k from 0 to n_P **do**
  if $k\Delta t_P < n_P\Delta t_P - \Delta\tau$ **then**
    calculate $x_P(t+k\Delta t_P)$ from $X_P(t-\Delta\tau)$ using linear interpolation
    append $x_P(t+k\Delta t_P)$ to $X_P^*(t)$
  else
    append $last\ element\ in\ X_P^*(t)$ to $X_P^*(t)$
  end
end

If a predictor is making accurate predictions of the human-driven vehicle's states, then the performance of the FAV controller should show a big improvement when delay handling situation is changed from the first case to the second.

III. Experimental Results and Analysis

In this section, the experimental results and analysis are presented. The setup of the experimental environment is introduced in III-A. The results of predictive control in the absence of communication constraints are presented and analyzed in III-B. The control results under the effect of propagation delay and packet loss are separately given in III-C and III-D. The results under a realist setup of communication constraints are presented and analyzed in III.E.

A. Experiment Setup

Since the control of an AV following another AV will be the same as conventional CAV control problem, in order to illustrate the core challenge in connected mixed traffic, we will focus on the most critical and most difficult AV control, which is to control the FAV to follow a HDV. We will use the performance of this FAV to demonstrate the results of anticipative and predictive Control.

According to our need, a three-vehicle simulation that consists of two AVs and one HDV is constructed. The driving simulator-based studies have been proven to be close to real vehicle studies [35], [36] and widely adopted by a number of researchers in the past [37], [38]. Using a driving simulator instead of a real vehicle can ensure the safety and ease

Authorized licensed use limited to: CLEMSON UNIVERSITY. Downloaded on July 11,2021 at 01:17:18 UTC from IEEE Xplore. Restrictions apply.

This article has been accepted for inclusion in a future issue of this journal. Content is final as presented, with the exception of pagination.

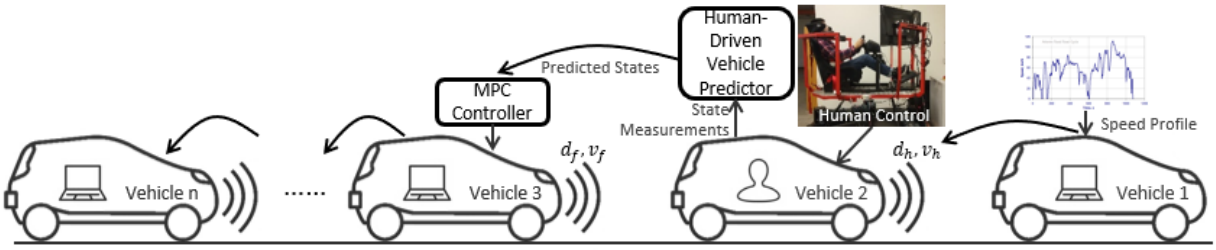

Fig. 2. Simulation setup.

the human driving experiments. Although the learnt human models in simulator-based studies and real vehicle based studies may be different due to the differences in human perception between the two types of studies, it does not affect the usability of the proposed approach because if it is proven to be effective in simulator-based studies, it would be applicable to real vehicle based studies too when used with real vehicle experimental data.

The system is shown in Fig. 2. While vehicle 1 is the LAV that simulates a free-flow driving case, vehicle 2 is the HDV that can be controlled by a human driver in real-time on a driving simulator with 6-DOF motion feedback. Given a reference trajectory to the LAV, we can anticipate its speed trajectory based on its known controller and share it with the following HDV. The HDV then uses this information to anticipates its trajectory and share it with the following AV. The HDV is built with complete longitudinal dynamics and the human driver needs to drive it to follow the LAV. Vehicle 3 is the FAV that is controlled by an MPC cruise controller. These three vehicles form a platoon. Each vehicle can measure its own speed and acceleration, while the HDV and FAV can additionally detect the headway distances and the speed of the vehicle in the front. Although the experiment in this paper only considers three vehicles, the size of the platoon is scalable. More automated vehicles, such as vehicle *n* in Fig. 2, can join the platoon and follow vehicle 2 further behind as long as they are within the V2V communication range. In this paper, the MPC problem is solved using ACADO toolkit [39].

In the experiment, the LAV is tracking three different driving cycles. The first one is the EPA Highway Fuel Economy Test Cycle (HWFET), which is a 12-minute-long mild highway cycle. The second is the Artemis Motorway 130 cycle which is an 18-minute-long aggressive motorway cycle with heavier braking and wider open throttle. The last one is the New York City Cycle (NYCC) with shortened stop time, which is an eight-minute-long urban driving cycle. The three cycles provide a variety of different driving behaviors for the LAV, which makes the comparison of the controller's performance more convincing. Three different human drivers (refer to as driver A, B and C hereafter) were required to drive the HDV in their preferred ways and maintain a comfortable distance from the LAV. One set of training data was collected when the LAV was following the HWFET cycle, and one set of testing data was collected when the LAV was following each of the HWFET, the Artemis, and the NYCC cycles. During the training process, the IDM, the ANN, and the IMPC predictors were trained using the training data. During the testing

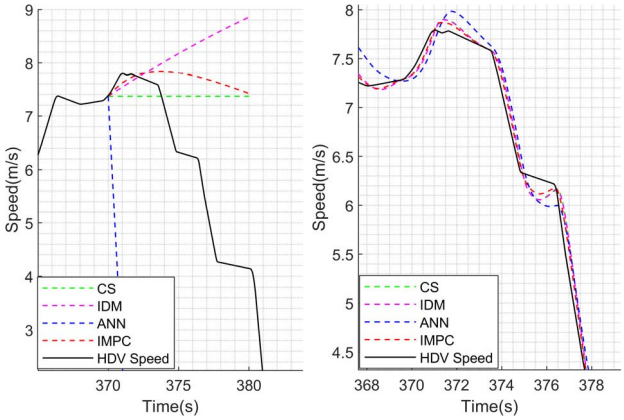

Fig. 3. Predictor performance for driver B under NYCC cycle.

process, the simulation reproduced the movement of the HDV using the testing data. In both the learning and the testing phases, the prediction horizon t_P was chosen to be 10 seconds and the prediction step size Δt_P was chosen to be 0.5 seconds for all predictors. The control frequency was 20Hz. The target headway distance d_f^{ref} was chosen to be 15 meters.

B. Predictive Control With Different Predictors in Ideal Situation

In this section, four predictors are coupled with the AV controller in order to identify which one can provide the smallest control error when there is no delay or packet loss in communication. This will reveal the theoretical potential of the IMPC predictor in connected automated driving. The results are shown in Table II, Fig. 3 and Fig. 4.

In Table II, blue and green colored values mark the best and the second best performers in that category. It can be clearly seen that the IMPC is doing the best in realizing the best headway tracking performance for the FAV. With the help of IMPC, the FAV manages to achieve not just the smallest mean absolute headway tracking error, but also the least prominent maximum and smallest errors for driver A under all three driving cycles. Since tracking headway distance is the only target considered by the MPC, such result indicates that the IMPC can maximize the performance of the FAV controller. It is worth mentioning that while the ANN predictor can achieve a level of mean tracking error that is similar to that of CS and IDM predictors under HWFET and Artemis cycles, its resulting mean tracking error under NYCC cycle is almost

Authorized licensed use limited to: CLEMSON UNIVERSITY. Downloaded on July 11,2021 at 01:17:18 UTC from IEEE Xplore. Restrictions apply.

This article has been accepted for inclusion in a future issue of this journal. Content is final as presented, with the exception of pagination.

TABLE II
MPC PERFORMANCE COMPARISON WITH DIFFERENT PREDICTORS, IDEAL SITUATION, DRIVER A

Cycle		HWFET			Artemis (Unseen Cycle)			NYCC (Unseen Cycle)		
Error Type	Predictor	Mean Abs. Value	Max. Value	Min. Value	Mean Abs. Value	Max. Value	Min. Value	Mean Abs. Value	Max. Value	Min. Value
Acceleration (m/s^2)	CS	0.3325	1.6430	-3.1692	0.5268	3.4344	-7.2628	0.5886	4.2969	-7.2768
	IDM	0.3308	1.6407	-3.1306	0.5199	3.3509	-6.9853	0.5823	3.8419	-6.9099
	ANN	0.3319	1.6589	-3.4083	0.5308	4.2698	-7.8194	0.6379	4.1579	-8.1919
	IMPC	0.3256	1.5342	-3.1934	0.5079	2.8463	-7.4645	0.5678	3.4305	-7.4514
Control Input (m/s^2)	CS	0.3397	2.0187	-3.1751	0.5410	4.8956	-7.3001	0.6170	5.0000	-7.3070
	IDM	0.3377	2.0156	-3.1443	0.5338	4.7144	-7.1513	0.6090	5.0000	-6.9376
	ANN	0.3389	2.0480	-3.4418	0.5481	5.0000	-8.3534	0.7099	5.0000	-8.3982
	IMPC	0.3321	1.8772	-3.2116	0.5209	3.8930	-7.5589	0.5923	4.5630	-7.4801
Tracking Error (m)	CS	0.0814	0.3237	-0.9536	0.1718	0.4705	-3.1503	0.4826	0.6405	-3.4292
	IDM	0.0731	0.3051	-0.7895	0.1489	0.4560	-2.9559	0.4076	0.6224	-2.8439
	ANN	0.0976	1.6429	-0.6679	0.2373	1.8741	-2.5510	1.0675	2.1630	-2.5566
	IMPC	0.0565	0.2337	-0.5201	0.1078	0.3326	-1.9520	0.3267	0.4612	-1.9750

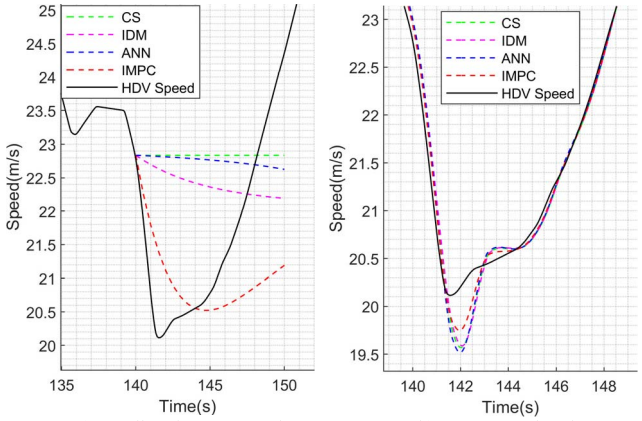

Fig. 4. Predictor performance for driver C under artemis cycle.

twice as large as those of the other predictors. That is because while the Artemis cycle is sharing some similarities with the HWFET cycle, the NYCC cycle is completely different from the other two cycles. Being trained from limited data collected from the HWFET cycle, the ANN can perform relatively well in a familiar environment. However, it loses functionality in a new environment.

The performance and the efforts of the FAV to track the target headway depends on the prediction accuracy of the HDV and the controller design. With an unsatisfied prediction and inappropriate controller design, the automated vehicle may not track the reference well, and the controls may also consume more energy. Therefore, although control input and vehicle acceleration are not considered in the cost function of the FAV's MPC controller, we have compared these indices between our proposed approach and existing approaches to show the advantage in saving energy consumption. Table II shows that the IMPC predictor is able to achieve lower average acceleration and control input for the FAV, which is equivalent to being more energy-efficient according to [28]. One may notice that the IMPC predictor sometimes causes a slightly larger maximum deceleration than the IDM and the CS predictors. When combined with the minimum tracking error performance, a larger maximum deceleration means

TABLE III
FIGURE LEGEND

Black Solid *	Red Solid ×	Red Dashed ×	Magenta Solid ◇	Magenta Dashed ◇	Blue Solid ○	Blue Dashed ○
CS	IDM w/o. T.S.	IDM w. T.S.	ANN w/o. T.S.	ANN w. T.S.	IMPC w/o. T.S.	IMPC w. T.S.

that the IMPC predictor makes the MPC controller to react more responsively to emergent brake events from the human-driven vehicle. Thus, in ideal situations, the IMPC is able to provide improved control accuracy, riding comfort and energy efficiency to the FAV. We observed similar results from driver B and driver C's experiment data.

Fig. 3 and Fig. 4 show two examples of how the predicted HDV speed versus the actual HDV speed looks like, and how the FAV changes its speed to HDV speed when different predictors are used. Fig. 3 shows one prediction for driver B under NYCC cycle. In Fig. 3 a), the IMPC is clearly generating the most accurate anticipation for the HDV. It can maintain the current motion trend of the HDV in a short horizon, as well as avoid deviating too much from the actual motion in a longer horizon. The IDM-based predictor is having much larger prediction errors in longer horizons. The ANN-based predictor is unable to make effective predictions in the NYCC cycle since the environment of the cycle is entirely different from that of the training data set. As a result, the HDV has the smoothest speed curve when anticipations from IMPC are available. Fig. 4 shows one prediction for driver C under Artemis cycle. IMPC is the only predictor that catches both the current deceleration and the future acceleration trends. Both the IDM and the ANN-based predictors tend to be not very sensitive in this situation. The HDV once again is having the smallest speed variation when IMPC anticipation is available.

C. Predictive Control With Different Predictors Under Different Propagation Delays

In this section, all four predictors are coupled with the MPC FAV controller when there are different propagation delays.

Authorized licensed use limited to: CLEMSON UNIVERSITY. Downloaded on July 11,2021 at 01:17:18 UTC from IEEE Xplore. Restrictions apply.

This article has been accepted for inclusion in a future issue of this journal. Content is final as presented, with the exception of pagination.

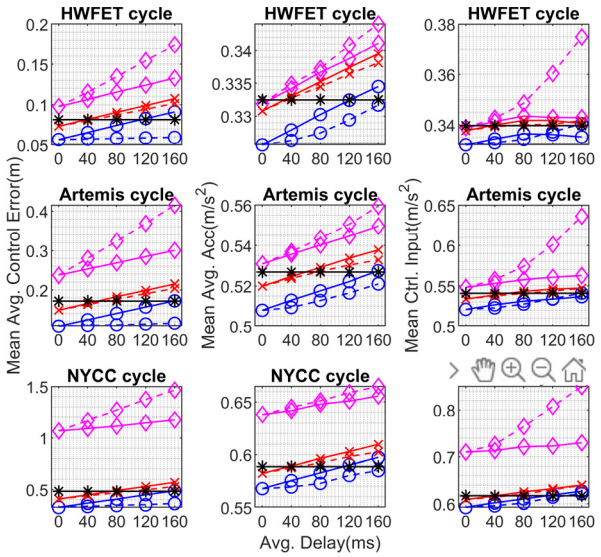

Fig. 5. Predictor performance under delays, driver A.

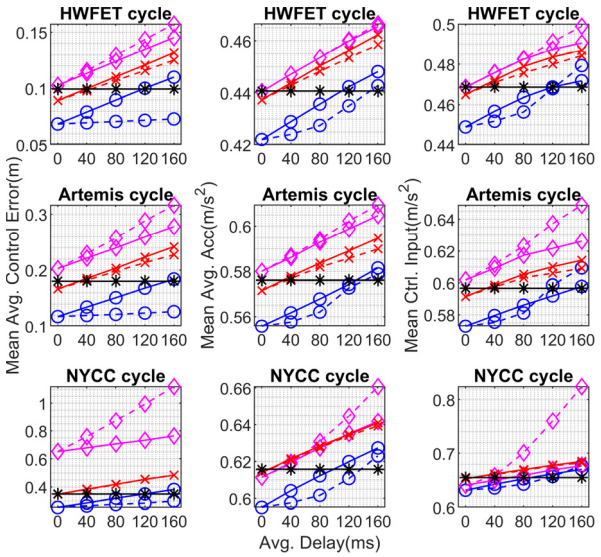

Fig. 6. Predictor performance under delays, driver B.

Literature [40] has pointed out that for close-range cooperative platooning, the total communication delay should not exceed 100ms. Existing communication protocols have been able to reduce the delay to below 20ms [41], [42]. In this paper, we explore the performance of the three predictors around and even beyond the 100ms delay limit. A random discrete-time time-varying propagation delay is added to the simulation in the form given by (19).

$$\Delta\tau = 0.5\Delta\tau_{avg} + \Delta\tau_{avg} \cdot U(0,1) \tag{19}$$

where $\Delta\tau_{avg}$ is the average value of the injected propagation delay, and $U(0,1)$ is a random number that obeys uniform distribution between 0 and 1. The range of injected delay in this paper is from $0.5\Delta\tau_{avg}$ to $1.5\Delta\tau_{avg}$. In this section we evaluated the predictors with $\Delta\tau_{avg} = 40, 80, 120$ and $160ms$. The results are of this shown in Fig. 5 to Fig. 7. The meanings of the different curves and marks in the figures are given in Table III.

Fig. 5 shows the performance of the MPC FAV controller when the predictions about driver A is shared with it. The CS predictor is not affected by the communication delay. In terms of tracking performance, The IDM predictor performs better than the CS predictor when the delay is low. However, when the average delay exceeds 40-80ms, the tracking accuracy worsens. Meanwhile, the IMPC predictor also shows a similar trend but with even better performance. The performance is superior to that of the CS predictor until the average delay reaches 120-160ms, while showing consistent advantage over the IDM predictor under all delays. The ANN predictor is having the worst tracking accuracy, especially under NYCC cycle, which again shows its disadvantage in handling unseen situations. When the timestamps of shared information are available and the prediction is corrected, both the IDM and the IMPC predictors experience improvements in their respective tracking accuracies. After delay compensation, the IMPC experiences a more noticeable improvement than the rest, eventually becoming better than all the other predictors under

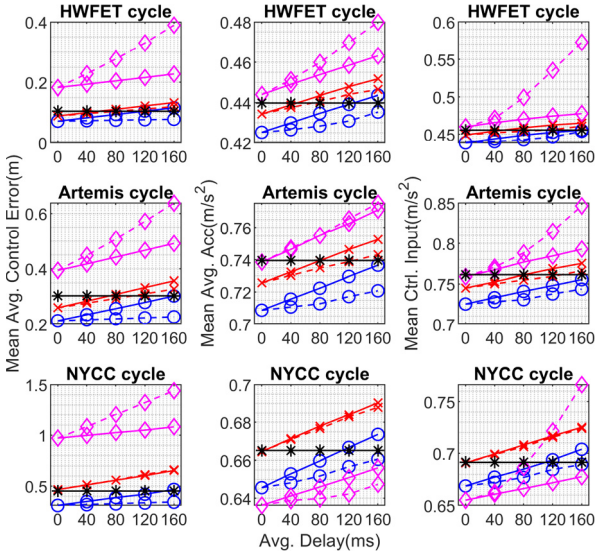

Fig. 7. Predictor performance under delays, driver C.

all types of delays. This indicates that IMPC can provide more accurate anticipations over the prediction horizon. The tracking accuracy from ANN predictor, on the other hand, is worsened when the timestamps are present. The ANN is not able to provide effective multi-step predictions, possibly because it is undertrained by the limited training data. Another reason behind the ineffectiveness of multi-step prediction is the unpredictable behavior of the network when it is presented with unseen situations. Average control input and vehicle acceleration are again shown in the figures to get more comprehensive comparisons between predictors. The average vehicle acceleration achieved by different predictors is showing a similar trend to the headway tracking error. The IMPC predictor is having a smaller mean acceleration, and handles large delays better when compared to the IDM and the ANN predictors. When timestamps are available, the IMPC can reduce the mean absolute acceleration the most. All these

Authorized licensed use limited to: CLEMSON UNIVERSITY. Downloaded on July 11,2021 at 01:17:18 UTC from IEEE Xplore. Restrictions apply.

This article has been accepted for inclusion in a future issue of this journal. Content is final as presented, with the exception of pagination.

phenomena mean that the IMPC predictor does not need to sacrifice riding comfort in order to improve the control accuracy of the FAV. When it comes to the average control input, the delay correction can cause the IMPC to have a larger average control input than when the timestamps are unavailable. However, when compared to other predictors, the control cost of the IMPC is still small as long as the average delay is below 120ms. Based on driver A's comparison result, we can conclude that the IMPC predictor can lead to the best headway tracking accuracy across all delay scenarios. Meanwhile, it does not need to sacrifice riding comfort or and energy efficiency when the average communication delay is below 120ms. It is reasonable to believe that the IMPC predictor can demonstrate consistent advantages in terms of both riding comfort and energy efficiency when the MPC is including corresponding primitive costs in the cost function.

Fig. 6 and Fig. 7 show the results from driver B and C. The overall trends of the results are observed to be similar to that of driver A. Since different drivers have different driving styles, the location of the crossing points of predictors' performance are different. For driver B, the IDM predictor cannot predict his action very accurately. It becomes worse than that of CS when the delay is merely about 30ms under the HWFET and the Artemis cycles, and falls behind that of CS almost all the time under the NYCC cycle. The correction with available timestamps does not seem to help much. The IMPC predictor once again handles a delay of 120ms well even without the timestamps. When the timestamps are available, the control errors are significantly reduced with almost no compromise on the control cost. For driver C, the IMPC predictor with timestamps correction can maintain its advantage in all three aspects even under an average communication delay of 160ms. On the contrary, the large headway tracking error proves that the ANN predictor is not working effectively.

Overall, the IMPC predictor can help the MPC controller of the FAV to achieve lower control error, better riding comfort and energy efficiency when the communication delay is under 120ms. Moreover, it reduces the control error even further when the global timestamps of the shared information are available.

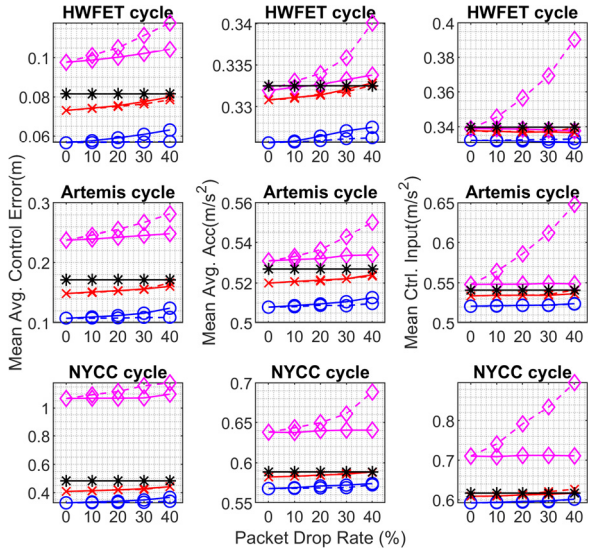

Fig. 8. Predictor performance under packet losses, driver A.

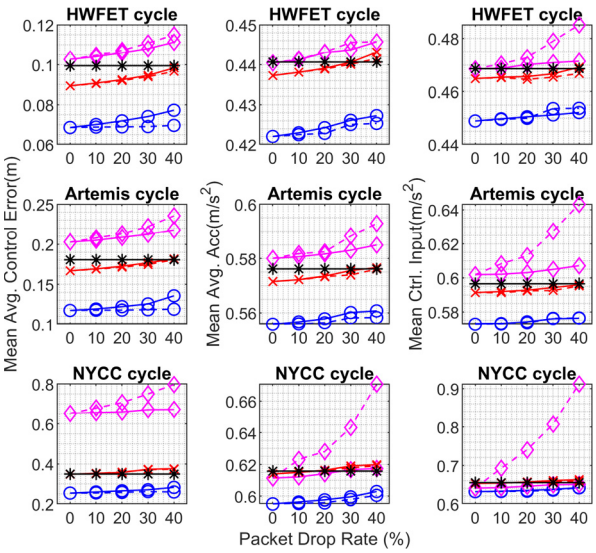

Fig. 9. Predictor performance under packet losses, driver B.

D. Predictive Control With Different Predictors Under Different Packet Loss Rates

In this section, all four predictors are coupled with the MPC FAV controller when there are different packet loss rates. Literature [43] has done a real-world reliability test for IEEE 802.11p-based V2V communication. Their data shows that the packet loss rate can be as high as 30% under line of sight communication. The range of packet loss rate in this paper is from 10% to 40%. The results are shown in Fig. 8 to Fig. 10.

In this section, the communication frequency is set to 20Hz. A 50ms equivalent delay will be imposed when a packet is lost. Even when a packet loss rate of 40% is applied, it is still rare to see three consecutive packets getting lost. Thus, theoretically, the impact of packet loss alone should be less obvious than that of delay. The figures confirm this guess. IDM, ANN, and IMPC-based predictors are all performing better under packet losses than under long delays. The IMPC predictor is having the best headway tracking accuracy among all three drivers under all packet loss scenarios. The IMPC predictor is achieving the best performance in terms of mean acceleration and mean control input among all the four predictors. Overall, the performance of the IMPC predictor is the best in terms of reducing the control error, improving riding comfort and energy efficiency under the presence of packet drops.

E. Predictive Control With Different Predictors Under Combination of Propagation Delays and Packet Losses

In this section, the performances of the four predictors under a realistic combination of propagation delay and packet loss is compared. Literature [10] suggests that the communication delay should be between one and two times of communication cycle time when there's no packet loss. In this section, the

Authorized licensed use limited to: CLEMSON UNIVERSITY. Downloaded on July 11,2021 at 01:17:18 UTC from IEEE Xplore. Restrictions apply.

This article has been accepted for inclusion in a future issue of this journal. Content is final as presented, with the exception of pagination.

TABLE IV

MPC PERFORMANCE COMPARISON WITH DIFFERENT PREDICTORS, UNDER DELAY AND PACKET LOSS, DRIVER A

Cycle		HWFET			Artemis (Unseen Cycle)			NYCC (Unseen Cycle)		
Error Type	Predictor	Mean Abs. Value	Max. Value	Min. Value	Mean Abs. Value	Max. Value	`Min. Value	Mean Abs. Value	Max. Value	Min. Value
Acceleration (m/s^2)	CS	0.3325	1.6430	-3.1692	0.5268	3.4344	-7.2628	0.5886	4.2969	-7.2768
	IDM	0.3393	1.7980	-3.6300	0.5382	3.6906	-7.5040	0.6096	4.3175	-7.3077
	IDM w/ TS	0.3377	1.7612	-3.3285	0.5334	3.5975	-7.3156	0.6041	4.0894	-7.0904
	ANN	0.3414	1.8376	-3.6076	0.5499	4.2405	-9.2993	0.6548	4.0922	-9.2680
	ANN w/ TS	0.3444	2.0233	-3.9616	0.5590	4.2381	-9.0439	0.6730	4.0535	-9.5149
	IMPC	0.3349	1.7266	-3.8922	0.5274	3.3245	-8.6621	0.5970	4.0475	-7.9793
	IMPC w/ TS	0.3321	1.6364	-3.3310	0.5217	2.9654	-7.6496	0.5848	3.6438	-7.5916
Control Input (m/s^2)	CS	0.3397	2.0187	-3.1751	0.5410	4.8956	-7.3001	0.6170	5.0000	-7.3070
	IDM	0.3445	2.4853	-4.6383	0.5517	5.0000	-9.1213	0.6404	5.0000	-7.9739
	IDM w/ TS	0.3431	2.3879	-3.6790	0.5486	5.0000	-8.1583	0.6399	5.0000	-7.6263
	ANN	0.3467	2.3088	-5.2962	0.5663	5.0000	-10.0000	0.7288	5.0000	-10.0000
	ANN w/ TS	0.3733	2.9414	-5.2200	0.6242	5.0000	-9.7160	0.8408	5.0000	-9.8649
	IMPC	0.3396	2.5037	-5.0634	0.5399	4.9143	-9.6229	0.6269	5.0000	-9.8903
	IMPC w/ TS	0.3415	2.0989	-4.1047	0.5427	4.2382	-10.0000	0.6208	4.9446	-7.9259
Tracking Error (m)	CS	0.0814	0.3237	-0.9536	0.1718	0.4705	-3.1503	0.4826	0.6405	-3.4292
	IDM	0.1081	0.4372	-1.1910	0.2189	0.6742	-4.0342	0.5678	0.9008	-3.8926
	IDM w/ TS	0.1023	0.6648	-1.1574	0.2052	0.7139	-3.8082	0.5319	0.8934	-3.5255
	ANN	0.1337	1.8483	-1.0519	0.3026	2.2453	-3.7978	1.1729	2.5704	-3.3737
	ANN w/ TS	0.1760	2.9791	-1.0260	0.4184	3.2974	-3.6969	1.4852	3.7844	-2.8701
	IMPC	0.0922	0.3786	-0.8768	0.1737	0.5535	-2.8346	0.4883	0.7185	-2.9147
	IMPC w/ TS	0.0593	0.2554	-0.5520	0.1156	0.3519	-2.2001	0.3641	0.4913	-2.2298

TABLE V

MPC PERFORMANCE COMPARISON WITH DIFFERENT PREDICTORS, UNDER DELAY AND PACKET LOSS, DRIVER B

Cycle		HWFET			Artemis (Unseen Cycle)			NYCC (Unseen Cycle)		
Error Type	Predictor	Mean Abs. Value	Max. Value	Min. Value	Mean Abs. Value	Max. Value	Min. Value	Mean Abs. Value	Max. Value	Min. Value
Acceleration (m/s^2)	CS	0.4406	2.1019	-6.0361	0.5761	4.0267	-7.5968	0.6158	3.9490	-6.7573
	IDM	0.4627	2.5081	-6.5346	0.5950	4.3790	-9.1725	0.6412	4.4614	-7.0886
	IDM w/ TS	0.4593	2.3799	-6.3430	0.5910	4.4238	-8.1936	0.6395	4.3000	-6.6416
	ANN	0.4668	2.5270	-6.3607	0.6046	4.0484	-9.7744	0.6424	2.8794	-8.0973
	ANN w/ TS	0.4675	2.5450	-6.2400	0.6123	4.1378	-9.9060	0.6654	4.0218	-7.6767
	IMPC	0.4493	2.2442	-7.6153	0.5802	3.7070	-8.8277	0.6277	4.1982	-8.0899
	IMPC w/ TS	0.4416	2.2915	-6.6182	0.5809	4.1461	-8.2431	0.6215	3.9207	-7.2399
Control Input (m/s^2)	CS	0.4686	3.6010	-6.1129	0.5966	5.0000	-7.6044	0.6553	5.0000	-6.8428
	IDM	0.4906	4.2323	-7.9260	0.6177	5.0000	-10.0000	0.6862	5.0000	-7.6574
	IDM w/ TS	0.4871	4.0673	-6.6963	0.6127	5.0000	-8.8161	0.6828	5.0000	-8.3191
	ANN	0.4952	4.3050	-7.4135	0.6292	5.0000	-10.0000	0.6787	4.0146	-9.5899
	ANN w/ TS	0.5034	4.3227	-6.8183	0.6518	5.0000	-10.0000	0.8181	5.0000	-9.8650
	IMPC	0.4776	3.5684	-8.1472	0.5994	5.0000	-10.0000	0.6709	5.0000	-8.8807
	IMPC w/ TS	0.4766	3.7031	-6.7404	0.6129	5.0000	-9.6576	0.6741	5.0000	-7.7270
Tracking Error (m)	CS	0.0994	0.3426	-1.5121	0.1805	1.4797	-3.3071	0.3495	0.6179	-2.2420
	IDM	0.1327	0.4769	-2.0819	0.2412	1.5329	-3.7352	0.4938	1.0336	-2.9853
	IDM w/ TS	0.1258	0.4640	-1.9175	0.2299	1.5298	-3.8896	0.4907	0.8771	-3.1678
	ANN	0.1471	0.5211	-2.0750	0.2782	2.2902	-4.5380	0.7666	2.3614	-2.0556
	ANN w/ TS	0.1591	0.5973	-2.0535	0.3194	3.6058	-4.4799	1.1169	3.2953	-1.4471
	IMPC	0.1118	0.4085	-1.4295	0.1863	1.4960	-2.5129	0.3837	0.7413	-2.0681
	IMPC w/ TS	0.0734	0.2706	-0.9395	0.1257	1.4626	-1.9540	0.2964	0.5129	-1.5621

communication frequency is set to 10Hz, which is a commonly used standard by dedicated short range communication (DSRC) [44]. The communication cycle time is then 100ms. Based on the measurements in [43], a packet loss rate of 20% is selected. The value of the loss rate is intentionally selected from the worse side in order to cover the nonideality in real V2V communication. The results are shown in Table IV to Table VI.

It can be seen that with delays and packet losses injected, all predictors except the CS predictor experienced a reduced performance when compared to the results given in Table II. Even the IMPC fails to deliver a smaller control error than that of the CS. However, when the timestamps are available, the performance of the IMPC predictor is improved significantly. In this case, the IMPC is having a big lead over other the predictors in terms of the average, the maximum and the minimum control errors for all drivers and under all cycles. Meanwhile, the IDM-based predictor has almost lost its functionality and is falling behind the CS-based predictor in almost every aspect. The ANN predictor is the only predictor for which the control accuracy worsens when delay compensation is available. The phenomena reflect that the IMPC is having

Authorized licensed use limited to: CLEMSON UNIVERSITY. Downloaded on July 11,2021 at 01:17:18 UTC from IEEE Xplore. Restrictions apply.

This article has been accepted for inclusion in a future issue of this journal. Content is final as presented, with the exception of pagination.

TABLE VI

MPC PERFORMANCE COMPARISON WITH DIFFERENT PREDICTORS, UNDER DELAY AND PACKET LOSS, DRIVER C

Cycle		HWFET			Artemis (Unseen Cycle)			NYCC (Unseen Cycle)		
Error Type	Predictor	Mean Abs. Value	Max. Value	Min. Value	Mean Abs. Value	Max. Value	Min. Value	Mean Abs. Value	Max. Value	Min. Value
Acceleration (m/s^2)	CS	0.4398	3.7490	-7.0280	0.7395	4.6749	-7.3431	0.6651	4.0394	-5.3079
	IDM	0.4523	3.5430	-7.6128	0.7532	4.8768	-7.8272	0.6907	4.4772	-5.7887
	IDM w/ TS	0.4468	3.2065	-7.3468	0.7431	4.8444	-7.3579	0.6898	4.4702	-5.7203
	ANN	0.4637	3.8814	-9.2782	0.7712	4.8106	-9.6361	0.6564	2.9155	-6.9499
	ANN w/ TS	0.4833	4.0955	-9.5833	0.7784	4.8545	-9.3725	0.6516	2.3783	-6.3594
	IMPC	0.4443	3.1206	-8.0295	0.7372	4.1298	-8.7574	0.6742	3.8157	-6.0165
	IMPC w/ TS	0.4355	2.5752	-7.6106	0.7206	3.4134	-7.7259	0.6606	3.3923	-5.2268
Control Input (m/s^2)	CS	0.4556	5.0000	-7.0757	0.7612	5.0000	-7.3536	0.6915	5.0000	-5.3134
	IDM	0.4678	5.0000	-9.6290	0.7767	5.0000	-10.0000	0.7255	5.0000	-6.1757
	IDM w/ TS	0.4612	4.5963	-7.9446	0.7664	5.0000	-8.3449	0.7247	5.0000	-6.4731
	ANN	0.4809	5.0000	-10.0000	0.7943	5.0000	-10.0000	0.6782	3.8966	-8.4186
	ANN w/ TS	0.5664	5.0000	-10.0000	0.8469	5.0000	-10.0000	0.7621	4.2617	-6.6391
	IMPC	0.4593	4.5927	-9.0051	0.7570	5.0000	-10.0000	0.7034	5.0000	-7.1511
	IMPC w/ TS	0.4546	3.6767	-7.9420	0.7430	5.0000	-8.3151	0.6894	4.6040	-5.3765
Tracking Error (m)	CS	0.1049	0.4218	-2.4176	0.3030	5.4237	-3.1008	0.4502	0.5901	-2.3969
	IDM	0.1349	0.4764	-2.1917	0.3596	5.5263	-3.8093	0.6518	0.9025	-3.3753
	IDM w/ TS	0.1211	0.5502	-1.6751	0.3287	5.5058	-3.7483	0.6682	0.8635	-3.4567
	ANN	0.2285	1.6553	-3.0422	0.4924	5.6004	-3.8096	1.0782	2.0776	-2.7858
	ANN w/ TS	0.3905	2.7191	-2.8780	0.6405	5.7201	-3.7779	1.4505	2.9508	-2.6772
	IMPC	0.1173	0.4129	-1.8682	0.3046	5.4748	-2.6583	0.4650	0.6381	-2.1152
	IMPC w/ TS	0.0784	0.2832	-1.2786	0.2271	5.3787	-2.0305	0.3433	0.4345	-1.5753

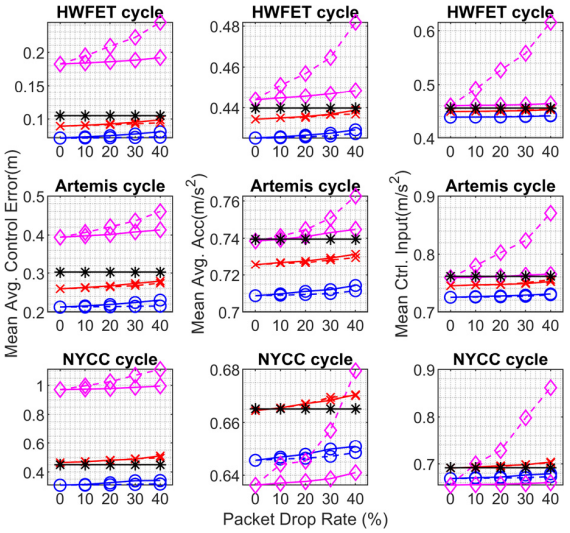

Fig. 10. Predictor performance under packet losses, driver C.

Abbreviation	Explanation
ANN	Artificial Neural Network
CA	Connected Vehicle
CS	Constant Speed
CV	Center Vehicle
FAV	Following Automated Vehicle
HDV	Human Driven Vehicle
IDM	Intelligent Driver Model
IMPC	Inverse Model Predictive Control
LAV	Lead Automated Vehicle
MPC	Model Predictive Control
w/ TS	With Timestamp

the most accurate prediction over the horizon, while the ANN's prediction is inaccurate and unstable.

It is worth mentioning that when such large delay exists in the system, the IMPC can no longer guarantee advantages in riding comfort or energy efficiency based on current controller. This is true even when the timestamps are available. Sometimes, the IMPC loses out to the CS by a small margin when it comes to vehicle acceleration and control input. However, considering the former's huge advantage in terms of control accuracy, it is very likely that the IMPC will regain its advantages in riding comfort and energy efficiency when these two aspects are considered by the predictive controller.

Overall, the combined communication delay and packet loss test proves that the IMPC-based predictor can bring actual benefits during real driving scenarios.

IV. CONCLUSION

In this paper a new IMPC-based approach is proposed to model and predict the longitudinal behaviors of human-driven vehicles in connected mixed traffic environments. Its predictions can be utilized by the model predictive control of following automated vehicles for improved control accuracy, riding comfort and energy efficiency. Comparisons are done between the IMPC-based and CS, IDM and ANN based predictive controller under random communication constraints. The results illustrate the effectiveness and the advantages of the proposed approaches in terms of handling delays and packet losses. It obviously outperforms other approaches when communication delays and packet losses are present. This is reflected in the lowest control error, average vehicle acceleration and average control input. With correction using the timestamps, the IMPC-based predictive controller can almost recover its performance under communication constrains to that in ideal situation.

As for future work, we plan to apply the current IMPC-based predictive controller to a larger platoon of vehicles to

Authorized licensed use limited to: CLEMSON UNIVERSITY. Downloaded on July 11,2021 at 01:17:18 UTC from IEEE Xplore. Restrictions apply.

This article has been accepted for inclusion in a future issue of this journal. Content is final as presented, with the exception of pagination.

study its effect on the large mixed traffic flow. We are also planning to use a more complex cost function design to more evidently reveal the differences in driving preferences between different drivers. In addition to the studied longitudinal driving, extending the proposed framework to the prediction and the control of other behaviors/states of connected mixed vehicles such as lane tracking and lane switching will also be further work to explore.

APPENDIX

See List of Abbreviations Table.

REFERENCES

[1] A. M. Pereira, H. Anany, O. Přibyl, and J. Přikryl, "Automated vehicles in smart urban environment: A review," in *Proc. Smart City Symp. Prague (SCSP)*, May 2017, pp. 1–8, doi: 10.1109/SCSP.2017.7973864.

[2] Y. Zhang, C. G. Cassandras, and A. A. Malikopoulos, "Optimal control of connected automated vehicles at urban traffic intersections: A feasibility enforcement analysis," in *Proc. Amer. Control Conf. (ACC)*, May 2017, pp. 3548–3553, doi: 10.23919/ACC.2017.7963496.

[3] Y. Rahmati and A. Talebpour, "Towards a collaborative connected, automated driving environment: A game theory based decision framework for unprotected left turn maneuvers," in *Proc. IEEE Intell. Vehicles Symp. (IV)*, Jun. 2017, pp. 1316–1321, doi: 10.1109/IVS.2017.7995894.

[4] S. Tsugawa, S. Kato, and K. Aoki, "An automated truck platoon for energy saving," in *Proc. IEEE/RSJ Int. Conf. Intell. Robots Syst.*, Dec. 2011, pp. 4109–4114, doi: 10.1109/iros.2011.6094549.

[5] L. Li and W. Ma, "A collision-free car-following model for connected automated vehicles," in *Proc. 96th Annu. Meet. Transp. Res. Board*, 2017, p. 3236, doi: 10.13140/RG.2.2.16083.27685.

[6] R. Dang, J. Ding, B. Su, Q. Yao, Y. Tian, and K. Li, "A lane change warning system based on V2 V communication," in *Proc. 17th Int. IEEE Conf. Intell. Transp. Syst. (ITSC)*, Oct. 2014, pp. 1923–1928, doi: 10.1109/ITSC.2014.6957987.

[7] J. I. Ge and G. Orosz, "Dynamics of connected vehicle systems with delayed acceleration feedback," *Transp. Res. C, Emerg. Technol.*, vol. 46, pp. 46–64, Sep. 2014, doi: 10.1016/j.trc.2014.04.014.

[8] S. E. Li *et al.*, "Dynamical modeling and distributed control of connected and automated vehicles: Challenges and opportunities," *IEEE Intell. Transp. Syst. Mag.*, vol. 9, no. 3, pp. 46–58, Sep. 2017, doi: 10.1109/MITS.2017.2709781.

[9] X. Liu, A. Goldsmith, S. S. Mahal, and J. K. Hedrick, "Effects of communication delay on string stability in vehicle platoons," in *Proc. IEEE Intell. Transp. Syst. (ITSC)*, Aug. 2001, pp. 625–630, doi: 10.1109/itsc.2001.948732.

[10] G. Orosz, "Connected cruise control: Modelling, delay effects, and nonlinear behaviour," *Vehicle Syst. Dyn.*, vol. 54, no. 8, pp. 1147–1176, Aug. 2016, doi: 10.1080/00423114.2016.1193209.

[11] F. Gao, S. E. Li, Y. Zheng, and D. Kum, "Robust control of heterogeneous vehicular platoon with uncertain dynamics and communication delay," *IET Intell. Transp. Syst.*, vol. 10, no. 7, pp. 503–513, Sep. 2016, doi: 10.1049/iet-its.2015.0205.

[12] H. An and J.-I. Jung, "Design of a cooperative lane change protocol for a connected and automated vehicle based on an estimation of the communication delay," *Sensors*, vol. 18, no. 10, p. 3499, Oct. 2018, doi: 10.3390/s18103499.

[13] S. E. Li, Y. Zheng, K. Li, L.-Y. Wang, and H. Zhang, "Platoon control of connected vehicles from a networked control perspective: Literature review, component modeling, and controller synthesis," *IEEE Trans. Veh. Technol.*, early access, Jul. 6, 2018, doi: 10.1109/TVT.2017.2723881.

[14] J. I. Ge and G. Orosz, "Optimal control of connected vehicle systems with communication delay and driver reaction time," *IEEE Trans. Intell. Transp. Syst.*, vol. 18, no. 8, pp. 2056–2070, Aug. 2017, doi: 10.1109/TITS.2016.2633164.

[15] D. Srinivasagupta, H. Schättler, and B. Joseph, "Time-stamped model predictive control: An algorithm for control of processes with random delays," *Comput. Chem. Eng.*, vol. 28, no. 8, pp. 1337–1346, Jul. 2004, doi: 10.1016/j.compchemeng.2003.09.027.

[16] C. M. J. Tampère, "Human-kinetic multiclass traffic flow theory and modelling. With application to advanced driver assistance systems in congestion," Ph.D. dissertation, Fac. Civil Eng. Geosci., Delft Univ. Technol., Delft, The Netherlands, 2004.

[17] M. Bando, K. Hasebe, A. Nakayama, A. Shibata, and Y. Sugiyama, "Dynamical model of traffic congestion and numerical simulation," *Phys. Rev. E, Stat. Phys. Plasmas Fluids Relat. Interdiscip. Top.*, vol. 51, no. 2, pp. 1035–1042, Feb. 1995, doi: 10.1103/PhysRevE.51.1035.

[18] A. Kesting and M. Treiber, "Calibrating car-following models by using trajectory data," *Transp. Res. Rec., J. Transp. Res. Board*, vol. 2088, no. 1, pp. 148–156, Jan. 2008, doi: 10.3141/2088-16.

[19] P. Angkititrakul, C. Miyajima, and K. Takeda, "Modeling and adaptation of stochastic driver-behavior model with application to car following," in *Proc. IEEE Intell. Vehicles Symp. (IV)*, Jun. 2011, pp. 814–819.

[20] A. Khodayari, A. Ghaffari, R. Kazemi, and R. Braunstingl, "A modified car-following model based on a neural network model of the human driver effects," *IEEE Trans. Syst., Man, Cybern. A, Syst. Humans*, vol. 42, no. 6, pp. 1440–1449, Nov. 2012, doi: 10.1109/TSMCA.2012.2192262.

[21] J. Morton, T. A. Wheeler, and M. J. Kochenderfer, "Analysis of recurrent neural networks for probabilistic modeling of driver behavior," *IEEE Trans. Intell. Transp. Syst.*, vol. 18, no. 5, pp. 1289–1298, May 2017, doi: 10.1109/TITS.2016.2603007.

[22] N. Bekiaris-Liberis, C. Roncoli, and M. Papageorgiou, "Predictor-based adaptive cruise control design," *IEEE Trans. Intell. Transp. Syst.*, vol. 19, no. 10, pp. 3181–3195, Oct. 2018, doi: 10.1109/TITS.2017.2771501.

[23] L. C. Davis, "Method of compensation for the mechanical response of connected adaptive cruise control vehicles," *Phys. A, Stat. Mech. Appl.*, vol. 562, Jan. 2021, Art. no. 125402, doi: 10.1016/j.physa.2020.125402.

[24] T. G. Molnar, W. B. Qin, T. Insperger, and G. Orosz, "Application of predictor feedback to compensate time delays in connected cruise control," *IEEE Trans. Intell. Transp. Syst.*, vol. 19, no. 2, pp. 545–559, Feb. 2018, doi: 10.1109/TITS.2017.2754240.

[25] M. Wang, S. P. Hoogendoorn, W. Daamen, B. van Arem, B. Shyrokau, and R. Happee, "Delay-compensating strategy to enhance string stability of adaptive cruise controlled vehicles," *Transportmetrica B, Transp. Dyn.*, vol. 6, no. 3, pp. 211–229, Jul. 2018, doi: 10.1080/21680566.2016.1266973.

[26] H. Xing, J. Ploeg, and H. Nijmeijer, "Compensation of communication delays in a cooperative ACC system," *IEEE Trans. Veh. Technol.*, vol. 69, no. 2, pp. 1177–1189, Feb. 2020, doi: 10.1109/TVT.2019.2960114.

[27] L. Guo and Y. Jia, "Modeling, learning and prediction of longitudinal behaviors of human-driven vehicles by incorporating internal human DecisionMaking process using inverse model predictive control," in *Proc. IEEE/RSJ Int. Conf. Intell. Robots Syst. (IROS)*, Nov. 2019, pp. 5278–5283, doi: 10.1109/IROS40897.2019.8968292.

[28] R. A. Dollar and A. Vahidi, "Efficient and collision-free anticipative cruise control in randomly mixed strings," *IEEE Trans. Intell. Veh.*, vol. 3, no. 4, pp. 439–452, Dec. 2018, doi: 10.1109/TIV.2018.2873895.

[29] S. Lefevre, C. Sun, R. Bajcsy, and C. Laugier, "Comparison of parametric and non-parametric approaches for vehicle speed prediction," in *Proc. Amer. Control Conf.*, Jun. 2014, pp. 3494–3499, doi: 10.1109/ACC.2014.6858871.

[30] A. Kesting, M. Treiber, and D. Helbing, "Enhanced intelligent driver model to access the impact of driving strategies on traffic capacity," *Phil. Trans. Roy. Soc. A, Math., Phys. Eng. Sci.*, vol. 368, no. 1928, pp. 4585–4605, Oct. 2010, doi: 10.1098/rsta.2010.0084.

[31] A. Ungoren and H. Peng, "An adaptive lateral preview driver model," *Vehicle Syst. Dyn.*, vol. 43, no. 4, pp. 245–259, Apr. 2005.

[32] C. Lv *et al.*, "Levenberg–Marquardt backpropagation training of multilayer neural networks for state estimation of a safety-critical cyber-physical system," *IEEE Trans. Ind. Informat.*, vol. 14, no. 8, pp. 3436–3446, Aug. 2018, doi: 10.1109/TII.2017.2777460.

[33] K. Mombaur, A. Truong, and J.-P. Laumond, "From human to humanoid locomotion—An inverse optimal control approach," *Auto. Robots*, vol. 28, no. 3, pp. 369–383, Apr. 2010, doi: 10.1007/s10514-009-9170-7.

[34] R. M. Lewis and V. Torczon, "Pattern search algorithms for bound constrained minimization," *SIAM J. Optim.*, vol. 9, no. 4, pp. 1082–1099, Jan. 1999.

[35] H. Bellem, M. Klüver, M. Schrauf, H.-P. Schöner, H. Hecht, and J. F. Krems, "Can we study autonomous driving comfort in moving-base driving simulators? A validation study," *Hum. Factors, J. Hum. Factors Ergonom. Soc.*, vol. 59, no. 3, pp. 442–456, May 2017, doi: 10.1177/0018720816682647.

[36] D. Llopis-Castelló, F. J. Camacho-Torregrosa, J. Marín-Morales, A. M. Pérez-Zuriaga, A. García, and J. F. Dols, "Validation of a low-cost driving simulator based on continuous speed profiles," *Transp. Res. Rec., J. Transp. Res. Board*, vol. 2602, no. 1, pp. 104–114, Jan. 2016, doi: 10.3141/2602-13.

Authorized licensed use limited to: CLEMSON UNIVERSITY. Downloaded on July 11,2021 at 01:17:18 UTC from IEEE Xplore. Restrictions apply.

This article has been accepted for inclusion in a future issue of this journal. Content is final as presented, with the exception of pagination.

[37] Y. Ali, A. Sharma, M. M. Haque, Z. Zheng, and M. Saifuzzaman, "The impact of the connected environment on driving behavior and safety: A driving simulator study," *Accident Anal. Prevention*, vol. 144, Sep. 2020, Art. no. 105643, doi: 10.1016/j.aap.2020.105643.

[38] Y. Ali, Z. Zheng, and M. M. Haque, "Connectivity's impact on mandatory lane-changing behaviour: Evidences from a driving simulator study," *Transp. Res. C, Emerg. Technol.*, vol. 93, pp. 292–309, Aug. 2018, doi: 10.1016/j.trc.2018.06.008.

[39] B. Houska, H. J. Ferreau, and M. Diehl, "ACADO toolkit—An open-source framework for automatic control and dynamic optimization," *Optim. Control Appl. Methods*, vol. 32, no. 3, pp. 298–312, May 2011, doi: 10.1002/oca.939.

[40] D. Reichardt, M. Miglietta, L. Moretti, P. Morsink, and W. Schulz, "CarTALK 2000: Safe and comfortable driving based upon inter-vehicle-communication," in *Proc. Intell. Vehicle Symp.*, vol. 2, Jun. 2002, pp. 545–550.

[41] K. Tokuda, M. Akiyama, and H. Fujii, "DOLPHIN for inter-vehicle communications system," in *Proc. IEEE Intell. Vehicles Symp.*, Oct. 2000, pp. 504–509, doi: 10.1109/ivs.2000.898395.

[42] M. Durresi, A. Durresi, and L. Barolli, "Emergency broadcast protocol for inter-vehicle communications," in *Proc. 11th Int. Conf. Parallel Distrib. Syst. (ICPADS)*, vol. 2, 2005, pp. 402–406, doi: 10.1109/ICPADS.2005.147.

[43] Y. Wang, J. Hu, Y. Zhang, and C. Xu, "Reliability evaluation of IEEE 802.11p-based vehicle-to-vehicle communication in an urban expressway," *Tsinghua Sci. Technol.*, vol. 20, no. 4, pp. 417–428, Aug. 2015, doi: 10.1109/TST.2015.7173456.

[44] J. B. Kenney, "Dedicated short-range communications (DSRC) standards in the united states," *Proc. IEEE*, vol. 99, no. 7, pp. 1162–1182, Jul. 2011, doi: 10.1109/JPROC.2011.2132790.

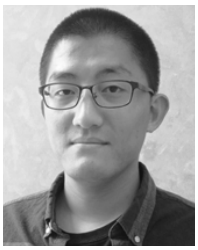

Longxiang Guo (Student Member, IEEE) received the B.S. degree in mechanical engineering from Tsinghua University, Beijing, China, in 2012, and the M.S. degree in mechanical engineering from the Chinese Academy of Sciences, Shenzhen, China, in 2015. He is currently pursuing the Ph.D. degree in automotive engineering with the Collaborative Robotics and Automation (CRA) Laboratory, Clemson University International Center for Automotive Research (CU-ICAR).

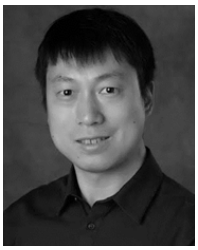

Yunyi Jia (Senior Member, IEEE) received the B.S. degree in automation from the National University of Defense Technology, Changsha, China, in 2005, the M.S. degree in control theory and control engineering from the South China University of Technology, Guangzhou, China, in 2008, and the Ph.D. degree in electrical engineering from Michigan State University, MI, USA, in 2014.

He is currently the Director of the Collaborative Robotics and Automation (CRA) Laboratory and the McQueen Quattlebaum Assistant Professor with the Department of Automotive Engineering, Clemson University, Greenville, SC, USA. His research interests include collaborative robotics, automated vehicles, and advanced sensing systems.

Authorized licensed use limited to: CLEMSON UNIVERSITY. Downloaded on July 11,2021 at 01:17:18 UTC from IEEE Xplore. Restrictions apply.